Effect of periodic roughness and surface defects on the terahertz scattering behavior of cylindrical objects

A. Jagannathan[a], A. J. Gatesman[a], T. Horgan[a], T. Goyette[a], M. Coloumbe[a], R. H. Giles[a], and W. E. Nixon[b]

[a]Submillimeter-Wave Technology Laboratory, University of Massachusetts Lowell, Lowell, MA 01854

[b]U.S. Army National Ground Intelligence Center, Charlottesville, VA 22911

ABSTRACT

This paper discusses the effect of periodic roughness and surface defects on the electromagnetic scattering of terahertz waves from cylindrical objects. The cylinders, possessing periodic roughness imparted during their fabrication process, had average roughness values ranging from approximately 0.1 μm – 0.50 μm. Metallic cylinders were fabricated from lathe-turned aluminum rods and dielectric cylinders were fabricated using a rapid prototype technique (stereolithography). The scattering behavior of the rough cylinders was measured in 160 GHz and 350 GHz compact radar ranges. In addition, the effect of seams and grooves on the scattering behavior of cylinders will also be presented.

Keywords: Terahertz, THz, Scattering, Rough Surfaces

1. INTRODUCTION

A firm understanding of the scattering behavior of terahertz (THz) waves is important for the development of remote sensing and imaging systems. Rough metallic surfaces will diffusely scatter electromagnetic radiation resulting in a reduction of specularly scattered radiation. By comparing the THz specular reflectance with scattering theory, non-destructive techniques for evaluation of a structure's surface roughness parameters have been demonstrated.[2,3] However, in applications such as Inverse Synthetic Aperture Radar (ISAR) imagery, the diffusely scattered radiation can cause unwanted artifacts. The primary objective of this paper is to investigate the effect of periodic roughness and surface defects on the THz scattering behavior of cylindrical objects by analyzing the objects ISAR imagery.

Roughness can be broadly classified as either random or periodic in nature. In this study, we restrict our analysis to periodic rough surfaces. Roughness is characterized in this paper by the average roughness R_a and periodicity P. Both conventional machining and rapid prototyping techniques such as stereolithography (SLA) tend to impart periodic roughness on cylindrical surfaces. In addition to periodic roughness, surface defects such as polished seams and unpolished grooves can also affect the ISAR imagery of an object and are investigated in this paper. Polished seams, as defined here, arise when distinct cylinders of the same diameter are physically attached together and then polished. The result can be a partial electrical discontinuity that can cause unwanted scattering artifacts. Grooves are tooling marks intentionally applied on a solid cylindrical surface.

2. SURFACE CHARACTERIZATION OF CYLINDERS

Three sets of cylinders were included in this study. Set 1 consisted of solid aluminum cylinders with periodic roughness created using conventional machining techniques. Set 2 consisted of aluminum coated dielectric cylinders with periodic roughness imparted during the SLA fabrication process. Set 3 consisted of solid aluminum cylinders with polished seams and unpolished grooves. Table 1 lists all cylinders used in this study. In addition to the cylinders listed in Table I, a polished reference cylinder with R_a of 0.02 μm was used as a comparison.

Report Documentation Page

Form Approved
OMB No. 0704-0188

1. REPORT DATE	2. REPORT TYPE	3. DATES COVERED
26 APR 2010		**00-00-2010 to 00-00-2010**

4. TITLE AND SUBTITLE	5a. CONTRACT NUMBER
Effect of periodic roughness and surface defects on the terahertz scattering behavior of cylindrical objects	5b. GRANT NUMBER
	5c. PROGRAM ELEMENT NUMBER
6. AUTHOR(S)	5d. PROJECT NUMBER
	5e. TASK NUMBER
	5f. WORK UNIT NUMBER
7. PERFORMING ORGANIZATION NAME(S) AND ADDRESS(ES) **University of Massachusetts Lowell,Submillimeter-Wave Technology Laboratory,Lowell,MA,01854**	8. PERFORMING ORGANIZATION REPORT NUMBER
9. SPONSORING/MONITORING AGENCY NAME(S) AND ADDRESS(ES)	10. SPONSOR/MONITOR'S ACRONYM(S)
	11. SPONSOR/MONITOR'S REPORT NUMBER(S)

12. DISTRIBUTION/AVAILABILITY STATEMENT
Approved for public release; distribution unlimited

13. SUPPLEMENTARY NOTES
SPIE Proceedings Vol. 7671 Terahertz Physics, Devices, and Systems IV, Mehdi Anwar, Nibir K. Dhar, Thomas W. Crowe, Editors, 26 April 2010

14. ABSTRACT
This paper discusses the effect of periodic roughness and surface defects on the electromagnetic scattering of terahertz waves from cylindrical objects. The cylinders, possessing periodic roughness imparted during their fabrication process, had average roughness values ranging from approximately 0.1 μm ? 0.50 μm. Metallic cylinders were fabricated from lathe-turned aluminum rods and dielectric cylinders were fabricated using a rapid prototype technique (stereolithography). The scattering behavior of the rough cylinders was measured in 160 GHz and 350 GHz compact radar ranges. In addition, the effect of seams and grooves on the scattering behavior of cylinders will also be presented.

15. SUBJECT TERMS

16. SECURITY CLASSIFICATION OF:			17. LIMITATION OF ABSTRACT	18. NUMBER OF PAGES	19a. NAME OF RESPONSIBLE PERSON
a. REPORT	b. ABSTRACT	c. THIS PAGE			
unclassified	**unclassified**	**unclassified**	**Same as Report (SAR)**	**12**	

Table I. List of cylinders used in the study.

Cylinder		Surface Characterization	Periodicity
Set 1 Lathe-turned solid metal Al	Solid Metal-1 Solid Metal-2 Solid Metal-3 Solid Metal-4 Solid Metal-5	$R_a \sim 0.08$ μm $R_a \sim 0.17$ μm $R_a \sim 0.34$ μm $R_a \sim 0.43$ μm $R_a \sim 0.48$ μm	100 μm
Set 2 Dielectric cylinders SLA "grown"	SLA-1	$R_a \sim 0.15$ μm	100 μm
	SLA-2	$R_a \sim 0.05$ μm	50 μm
Set 3 Solid metal cylinders with defects	Groove	Solid metal cylinders with two grooves	N/A
	Seam	Solid metal cylinders with two seams	

All cylinders used in this study were 8 inches long and measured 1.5 inches in diameter. The first set of cylinders used in this study was made from solid aluminum and had R_a values ranging from approximately 0.02 μm to 0.50 μm. The reference cylinder ($R_a \sim 0.02$ μm) and the roughest cylinder ($R_a \sim 0.48$ μm) are shown in Figure 1.

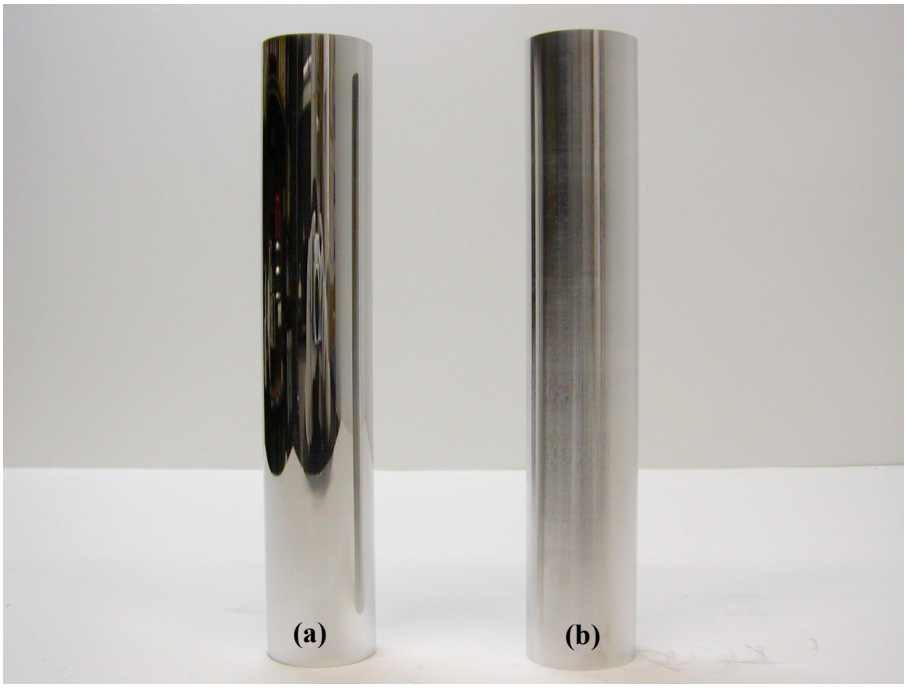

Figure 1. (a) Reference cylinder ($R_a \approx 0.02$ μm), and (b) Roughest cylinder ($R_a \approx 0.48$ μm).

The surface profile of the cylinders was measured using a Taylor Hobson stylus profilometer. The stylus traversed a distance of approximately 10 mm to obtain the surface profile. The raw uncalibrated surface profiles of the reference and roughest cylinders are shown in Figure 2. The surface profiles were post-processed with calibration data to get the stated R_a values shown in Table I. The periodic nature of the surface profile of the roughest cylinder is clearly evident.

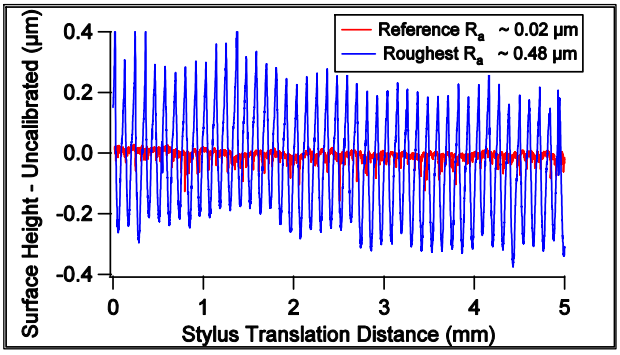

Figure 2. Surface profile of the polished (red curve) and roughest lathe-turned cylinder (blue curve) demonstrating the periodic nature of the surface roughness.

The second set of cylinders used in this study consisted of two metal-coated dielectric cylinders "grown" using SLA techniques. SLA-1 had a periodicity P = 100 µm and SLA-2 had a periodicity of P = 50 µm. Both cylinders were coated with aluminum using vacuum deposition techniques. Cylinder SLA-1 had a R_a of 0.15 µm and cylinder SLA-2 had a R_a of 0.05 µm. Cylinder SLA-1 is shown in figure 3 and the surface profile of both SLA cylinders is shown in figure 4. The periodic nature of the shorter period (higher frequency) surface roughness of cylinder SLA-2 is not evident from the surface profile. This might be due to the limitation of the profilometer in resolving high frequency roughness. Hence, the measured value of R_a of 0.05 µm for SLA-2 may be underestimated.

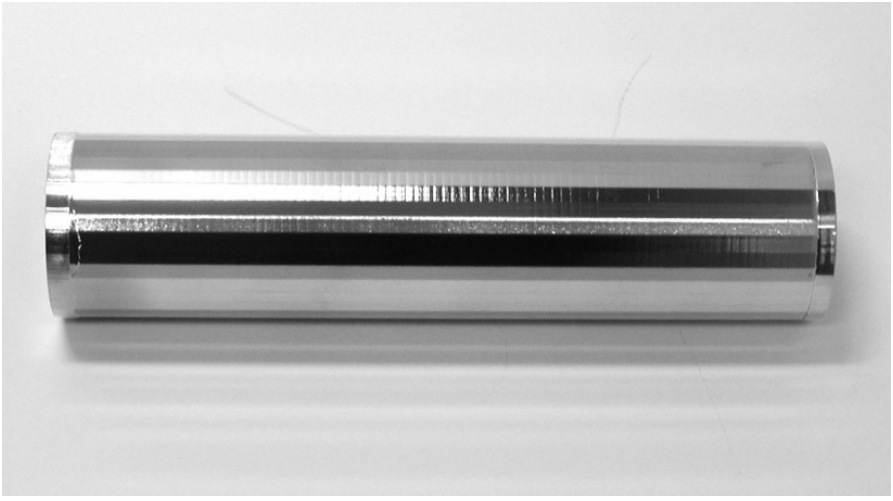

Figure 3. Dielectric cylinder SLA-1 (P = 100 µm and R_a = 0.15 µm) made using SLA techniques and coated with an Al thin film. The periodic roughness imparted to the surface during the SLA growth process can be seen.

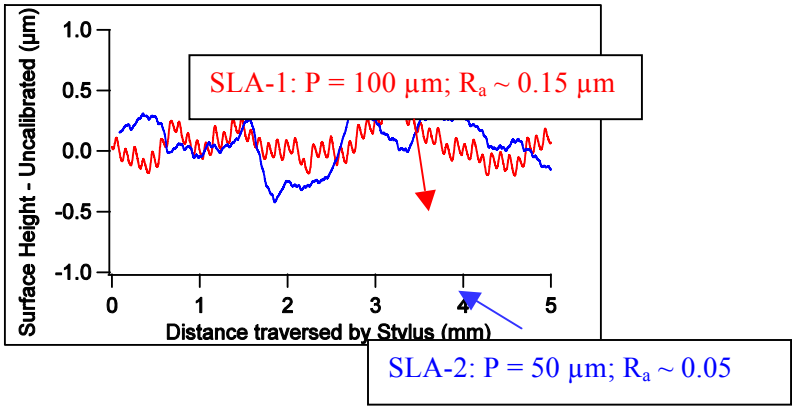

Figure 4. Surface profile of Al coated dielectric cylinders, SLA-1 (red curve) and SLA-2 (blue curve).

The third set of cylinders used in this study was comprised of solid aluminum cylinders with seams and grooves. An 8-inch-long cylinder with two seams was created by joining three cylinders with set screws, thereby creating partial electrical discontinuities (Fig. 5). The cylinder was then polished to determine if this would eliminate scattering behavior observed in unpolished cylinder measurements in a prior study. Another cylinder, similar to the one shown in figure 5, was made with grooves. Grooves were made by taking a single 8-inch-long cylinder and inscribing a tool mark on its surface. The cylinder with grooves is shown in figure 5. Since polished seams were difficult to observe, its cylinder is not shown here. The surface profile of the cylinders is shown in figure 6. The depth of the grooves is approximately 0.28 µm.

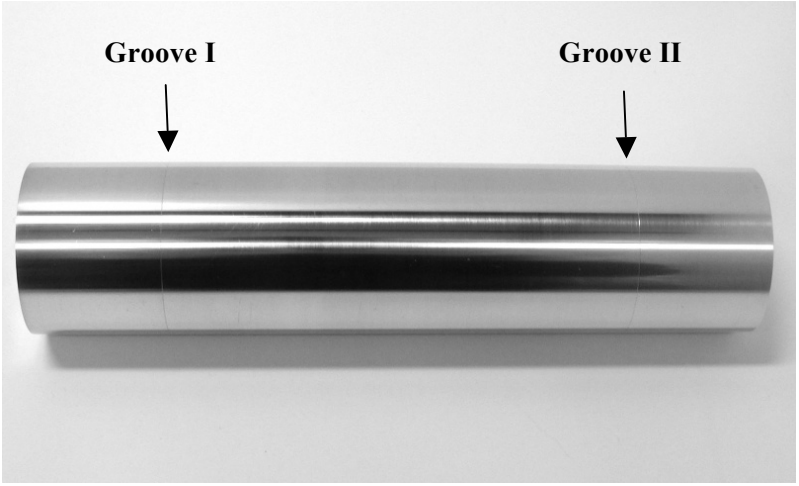

Figure 5. 8-inch-long Al cylinder with grooves at 1.5 in. from each end.

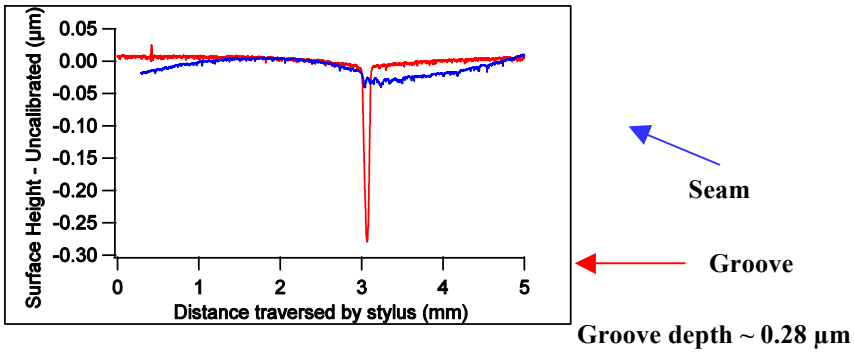

Figure 6. Surface profile of cylinders with grooves (red) and seams (blue).

3. MEASUREMENT SYSTEM DESCRIPTION

The scattering behavior of cylinders was collected using 160 GHz and 350 GHz fully polarimetric compact radar ranges. The schematic of the 160 GHz range is shown in figure 7. The 160 GHz range consisted of a solidstate transceiver, a main collimating antenna, a target positioning system, and a data acquisition system.[4,5] The cylinders were mounted on a support pylon using a dielectric saddle. One of the cylinders mounted on the pylon is shown in figure 8. The target positioning system automated the rotation of the cylinder's azimuthal angle. The 350 GHz compact radar, unlike the 160 GHz range, was based on a molecular gas laser system. The schematic of the 350 GHz range is shown in figure 9 and a detailed overview of the system can be found in Ref. [6].

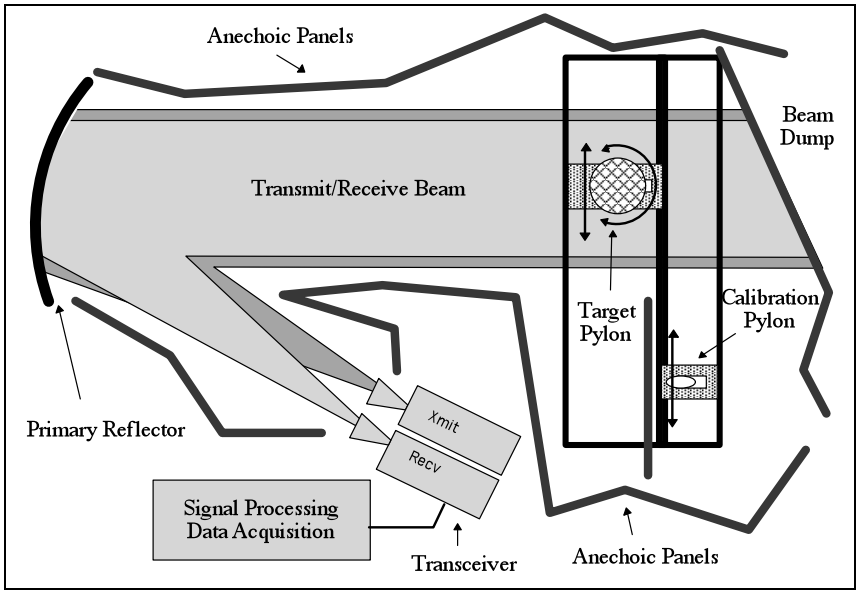

Figure 7. Schematic of the 160 GHz compact radar range.

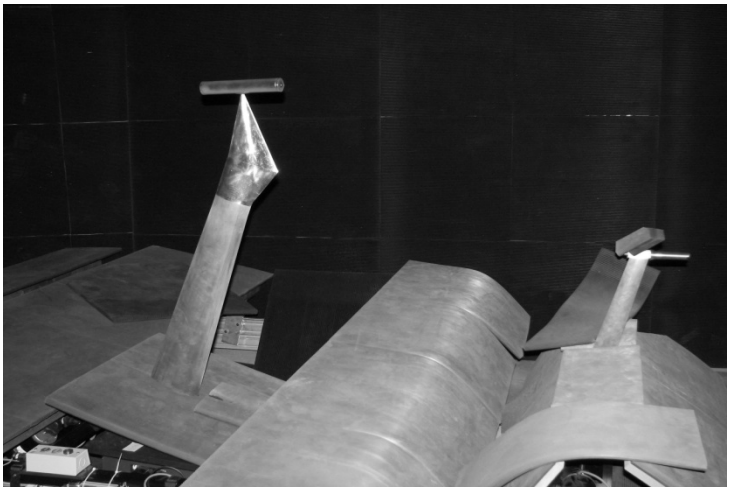

Figure 8. Cylindrical target placed on the pylon for measurement of scattering behavior. The shorter pylon shown on the right was an in-scene calibrated object used during the measurements.

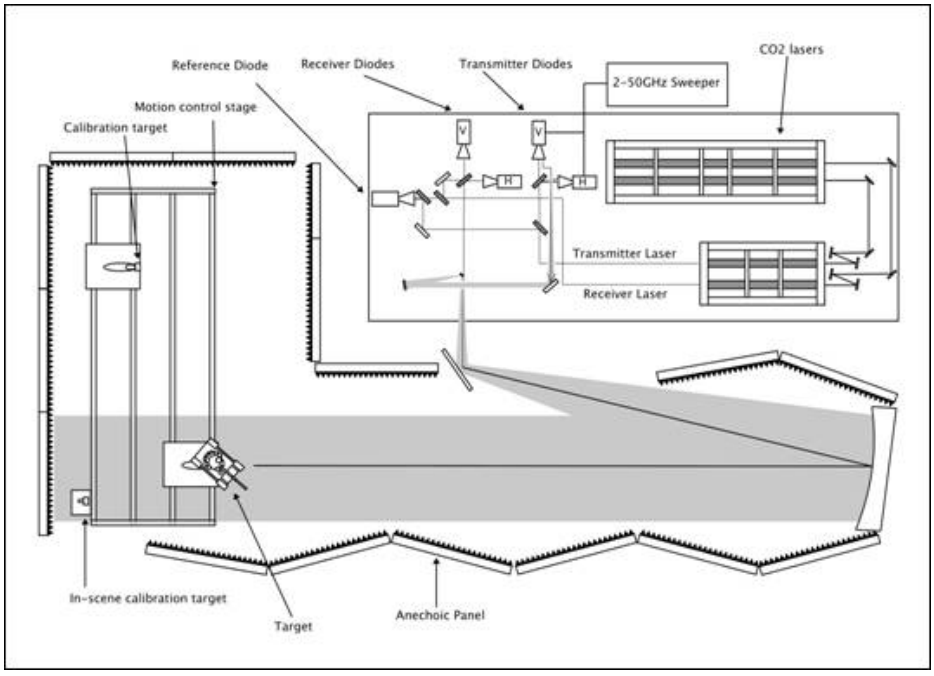

Figure 9. Schematic of the 350 GHz compact radar range.

4. EXPERIMENTAL RESULTS

The cylinder's polarimetric horizontal polarization (HH), vertical polarization (VV), and cross polarization (HV and VH) scattering behavior were obtained. HH polarization data appeared similar to that of VV polarization, therefore only HH polarization is presented in this paper. Discussion of the HV and VH scattering behavior of the cylinders is outside the scope of this paper. The measurements were taken at 0 degrees elevation and through a complete 360 degree azimuthal spin. Azimuth angle is defined such that at 90 degrees azimuth, the target was illuminated broadside. ISAR imagery was generated using standard processing techniques described in ref [5]. ISAR imagery is shown in figures 10-18. The numbers in the color maps are in units of dBsm.

4.1 ISAR Imagery at 160 GHz

4.1.1 Set 1 – Solid metal cylinders at 160 GHz

The ISAR images of the rough cylinders at 160 GHz were compared with the reference cylinder to study the effect of roughness on the ISAR imagery. No scattering artifacts were observed for the set of rough metallic cylinders Solid Metal-1 to Solid Metal-5 over the complete azimuthal angular range. Figure 10 shows the ISAR image of the reference cylinder and the roughest cylinder Solid Metal-5 at 45 degrees azimuth. The dotted lines in fig. 10 shows the approximate orientation of the cylinder. Throughout the 360 degree azimuthal spin, the ISAR images of the two cylinders looked virtually identical. The scattering features observed in figure 10 were due to scattering from the ends of the cylinder and from the support pylon at the center.

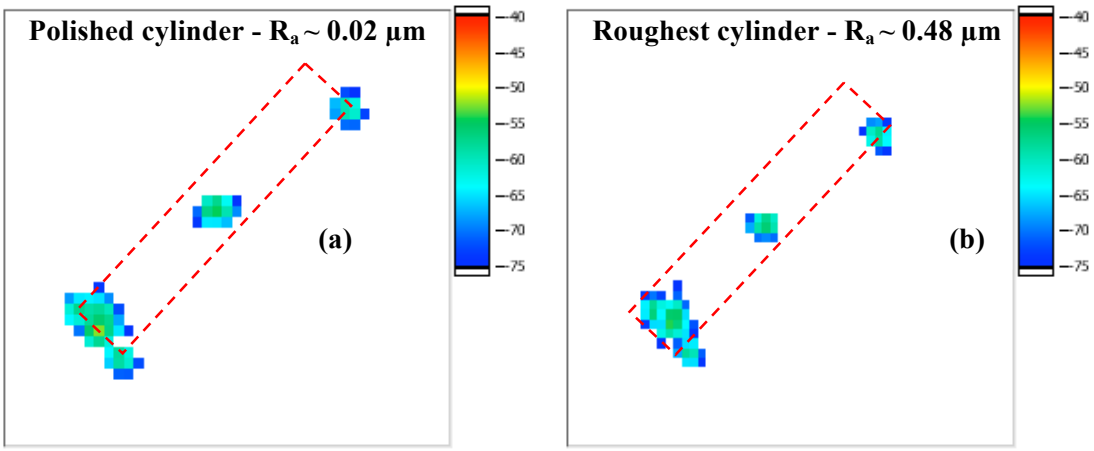

Figure 10. 160 GHz ISAR imagery at 45 degrees azimuth of a) Polished cylinder, and b) Solid Metal-5.

4.1.2 Set 2 – SLA grown cylinders at 160 GHz

The ISAR images of SLA fabricated cylinders, SLA-1 and SLA-2, were also compared with the reference polished cylinder. Scattering artifacts due to periodic roughness were observed in both cylinders. For cylinder SLA-1 with low frequency roughness, scattering artifacts were observed at 23 degrees azimuth in the -70 dBsm to - 79 dBsm range (see Fig. 11).

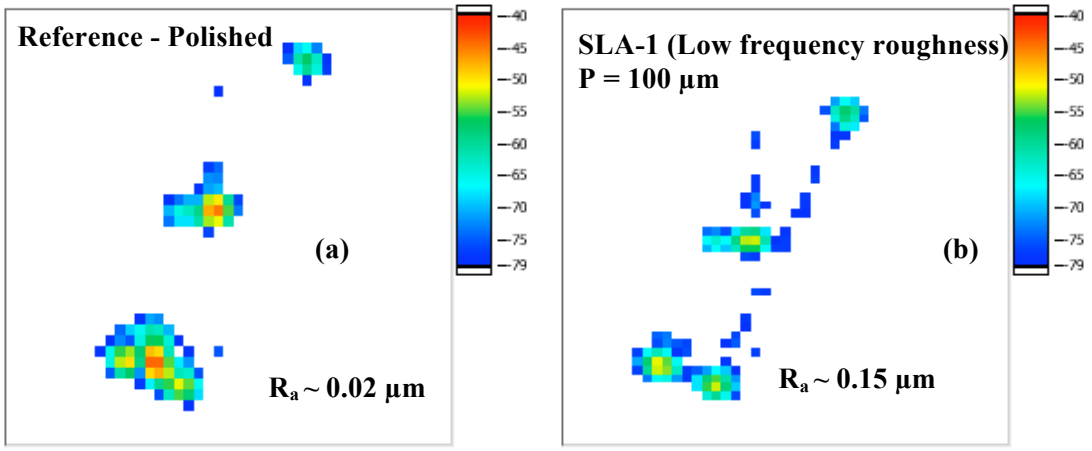

Figure 11. 160 GHz ISAR imagery at 23 degrees azimuth of a) Reference cylinder, and b) SLA-1.

For cylinder SLA-2 with high frequency roughness, scattering artifacts were observed at 40 degrees azimuth in the -65 dBsm to - 70 dBsm range (Fig. 12). Note that the scattered intensity for SLA-2 is higher than SLA-1.

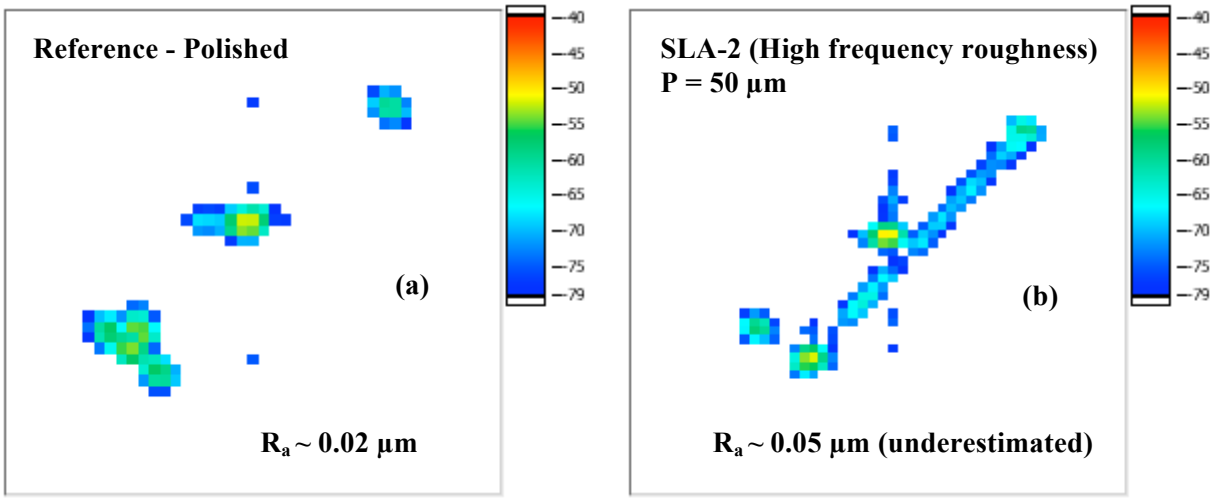

Figure 12. 160 GHz ISAR imagery at 40 degrees azimuth of a) Reference cylinder, and b) SLA-2.

4.1.3 Set 3 – Cylinders with seams and grooves at 160 GHz

The ISAR imagery of the cylinder with grooves did not show any scattering artifacts and therefore is not shown here. For the cylinder with polished seams, scattering artifacts (Fig. 13) were observed at 83 degrees azimuth at approximately the -65 dBsm level. The presence of polished seams in the ISAR image is indicated in Fig. 13b with red circles. Even though the seams were polished and difficult to observe visually, there presence were easily detected in the THz imagery

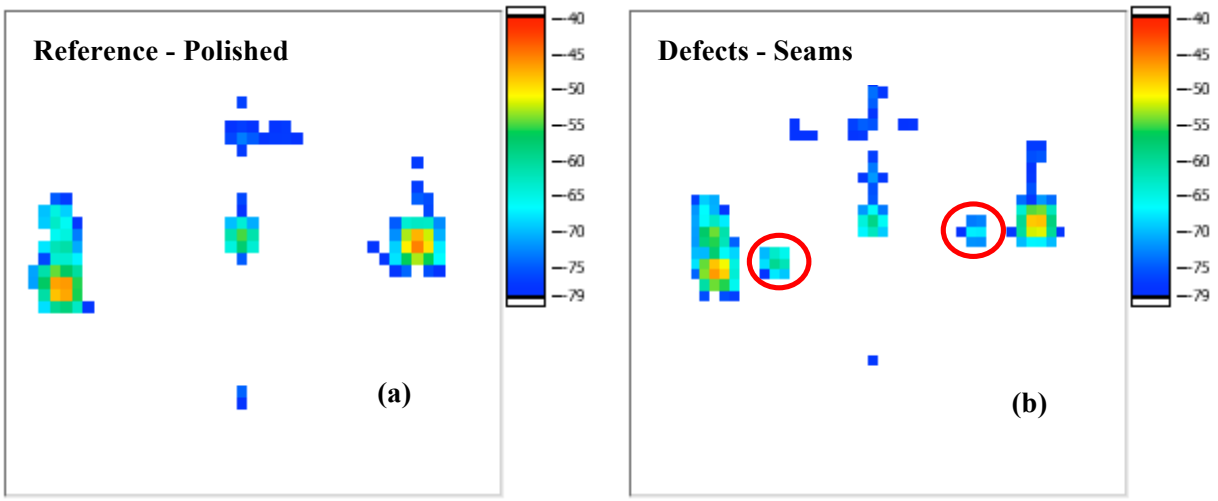

Figure 13. 160 GHz ISAR imagery at 83 degrees azimuth of a) Reference cylinder, and b) a cylinder with polished seams indicated by red circles.

4.2 ISAR Imagery at 350 GHz

4.2.1 Set 1– Solid Metal Cylinders at 350 GHz

Scattering artifacts were not observed at 350 GHz for any of the solid metal cylinders in Set 1. This result is similar to the observations made using the 160 GHz radar range.

4.2.2 Set 2– SLA grown cylinders at 350 GHz

In cylinder SLA-1 with low frequency roughness, made using SLA techniques, scattering artifacts were observed at 79 degrees azimuth at approximately the - 65 dBsm level (Fig. 14). In cylinder SLA-2 with high frequency roughness, scattering artifacts were observed at 70 degrees azimuth at approximately the - 60 dBsm level (Fig. 15).

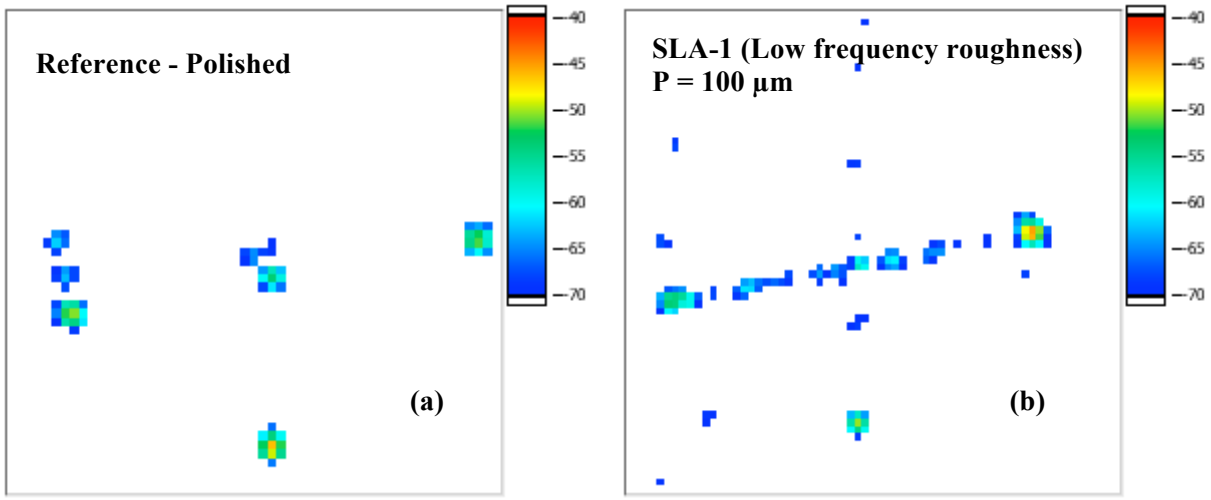

Figure 14. 350 GHz ISAR imagery at 79 degrees azimuth of a) Reference cylinder, and b) SLA-1.

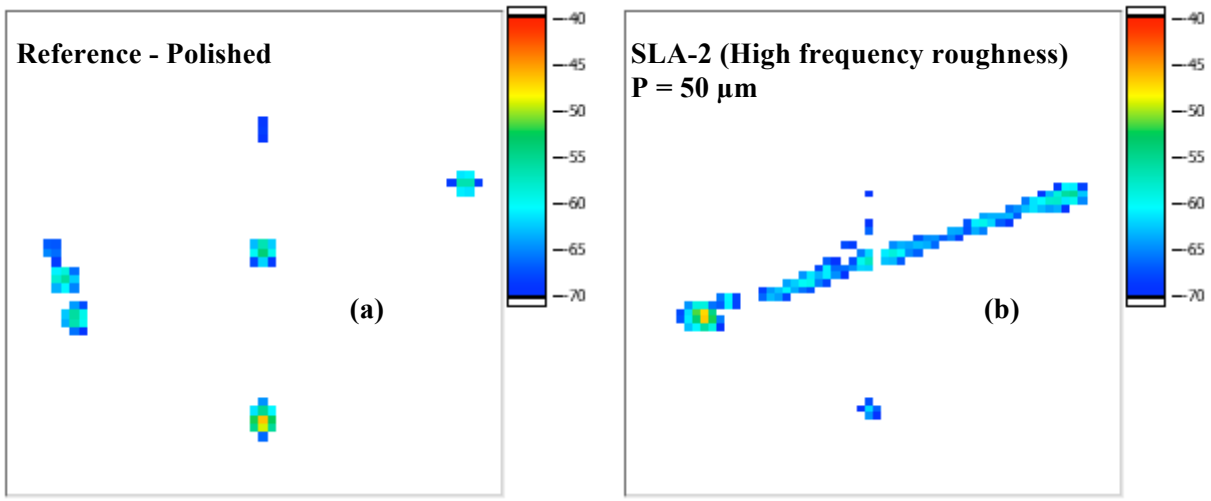

Figure 15. 350 GHz ISAR imagery at 70 degrees azimuth of a) Reference cylinder, and b) SLA-2.

4.2.3 Set 3 – Cylinders with seams and grooves at 350 GHz

Figure 16 and Figure 17 shows 350 GHz ISAR imagery of cylinders with grooves and polished seams, respectively. For the cylinder with grooves, the scattering artifacts were observed at 35 degrees azimuth in the -65 dBsm to -70 dBsm range. For the cylinder with polished seams, scattering artifacts were observed at 87 degrees azimuth in the -60 dBsm to -65 dBsm range. The ISAR image of reference cylinder is also shown for comparison.

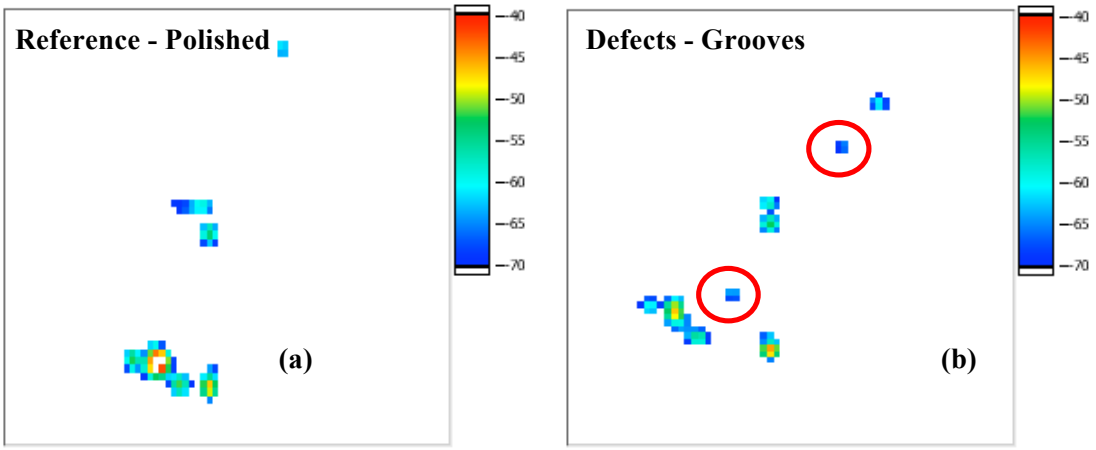

Figure 16. 350 GHz ISAR imagery at 35 degrees azimuth of a) Reference cylinder, and b) cylinder with grooves indicated by red circles.

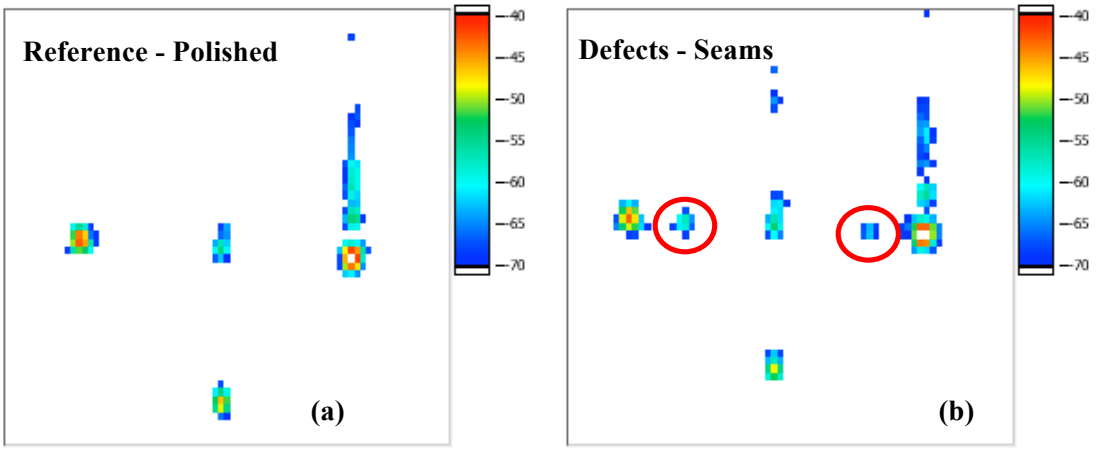

Figure 17. 350 GHz ISAR imagery at 87 degrees azimuth of a) Reference cylinder, and b) cylinder with polished seams indicated by red circles.

5. DISCUSSION

Metal coated dielectric cylinders created using SLA techniques had periodic roughness that significantly affected both the 160 GHz and 350 GHz data. From the ISAR imagery of the SLA cylinders, it is evident that even periodic roughness of R_a as low as 0.15 µm ($Ra/\lambda \sim 11{,}000$) can impact the ISAR imagery of the target. Interestingly, metallic cylinders with periodic roughness created using conventional lathe techniques having roughness almost three times that of cylinders made using SLA techniques did not affect the ISAR imagery of the cylinders**.** This prompted further study of other cylindrical surfaces with R_a of approximately 0.5 µm and with different periodicities and surface textures. One of the cylinders tested (designated here as cylinder SM-X), whose data are shown in Fig. 18, did show 160 GHz scattering artifacts in its ISAR image at 48 degrees azimuth in the -65 dBsm to -70 dBsm range. The ratio R_a/λ at 160 GHz for both cylinders is approximately 1/3750. Figure 19 compares the surface profile of the roughest cylinder

(Solid Metal-5) used in this study and cylinder SM-X. Though the R_a values of Solid Metal-5 and SM-X were approximately the same, other aspects of their profiles (such as period and texture) were substantially different. This indicates that scattering artifacts can be influenced by factors other than R_a.

The experimental results further showed that cylinders with seams affected the ISAR imagery. Grooves caused scattering artifacts in the ISAR image at 350 GHz, but not in 160 GHz. This might be due to the higher resolution of the ISAR images obtained in the 350 GHz system than the 160 GHz system.

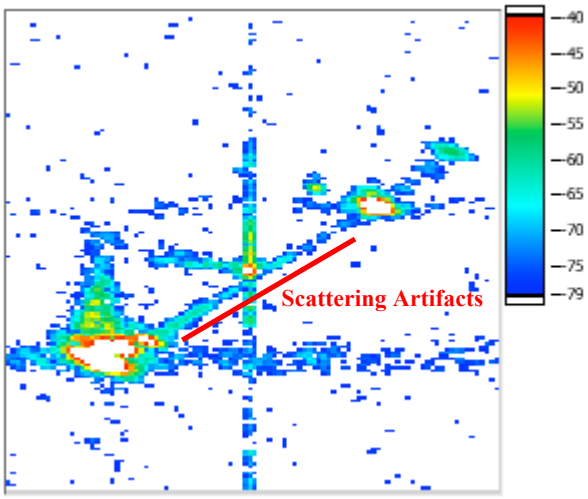

Figure 18. 160 GHz ISAR imagery at 48 degrees azimuth of cylinder SM-X with average roughness R_a of 0.50 µm. Rough surface scattering from the roughest cylinder prepared for this study (SM-5) with an $R_a \sim 0.48$ µm was not observed indicating that R_a/λ ratios alone cannot be used to predict if a cylindrical object will exhibit rough surface scattering.

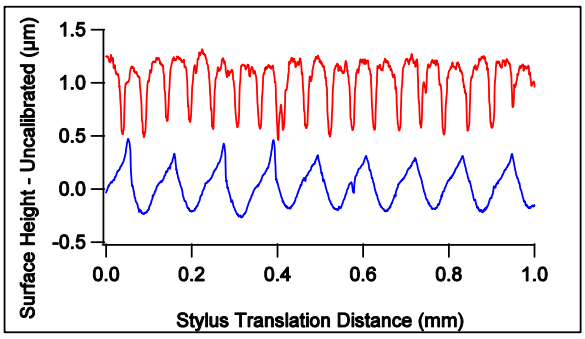

Figure 19. Comparison of surface profiles of cylinder SM-5 (blue) with R_a of 0.48 µm in which scattering artifacts were not observed and cylinder SM-X (red) with R_a of 0.5 µm in which scattering artifacts were observed on ISAR imagery. The cylinders have nearly the same R_a, but different periodicities and overall texture.

The benefits that can be derived from this study are two-fold. First, it empirically shows how minor surface features can affect the THz scattering behavior of metallic objects. Second, it identifies THz imaging systems as a potential candidate in the field of non-destructive testing. The sensitivity of such systems, if properly utilized, can be used to inspect sensitive structures (e.g. aircraft wings, rotors, and fuselage) for surface imperfections. The property of terahertz waves to be transparent to dielectric materials such as paints further favors the use of this technology for practical non-destructive applications.

CONCLUSION

In this paper, we have experimentally studied the effect of surface roughness and surface defects on the ISAR imagery of cylindrical objects. The ISAR imagery of the cylinders were obtained in two different compact radar ranges with center frequencies of 160 GHz and 350 GHz. Scattering artifacts were observed on ISAR imagery of cylinders made using SLA techniques with R_a as low as 0.15 μm ($R_a/\lambda \sim 1/11000$). In summary, we have demonstrated that scattering behavior of submicron roughness can be observed in THz imagery. In addition, this work identifies THz imaging as a potential candidate for non-destructive evaluation techniques.

ACKNOWLEDGEMENT

This work was supported by the National Ground Intelligence Center under US Army contract W911W4-06-C-0020.

REFERENCES

[1] P. Beckmann and A. Spizzichino, “The Scattering of Electromagnetic Waves from Rough Surfaces,” Artech House, 1987, pp. 80–98.

[2] Robert F. Anastasi and Eric I. Madaras “Terahertz NDE for Metallic Surface Roughness Evaluation,” Proceedings of the 4th International Workshop on Ultrasonic and Advanced Methods for Nondestructive Testing and Material Characterization, June 19, 2006.

[3] A. Jagannathan, A. J. Gatesman, and R. H. Giles, “Characterization of roughness parameters of metallic surfaces using terahertz reflection spectra,” Optics Letters, Vol. 34, No. 13, July 1, 2009.

[4] M. Coulombe, T. Horgan and J. Waldman, J. Neilson, S. Carter, and W. Nixon, ”A 160 GHz Polarimetric Compact Range for Scale Model RCS Measurements,” Antenna Measurements and Techniques Association (AMTA) Proceedings, Seattle, WA, pg 239, 1996.

[5] M. Coulombe, J. Waldman, R. Giles, A. Gatesman, T. Goyette, and W. Nixon, “Submillimeter-Wave Polarimetric Compact Ranges for Scale-Model Radar Measurements,” Microwave Symposium Digest, 2002 IEEE MTT-S International Vol. 3, 1583-1586, 2002.

[6] Thomas M. Goyette, Jason C. Dickinson, William J. Gorveatt, Jerry Waldman, William E. Nixon , "X-band ISAR imagery of scale-model tactical targets using a wide-bandwidth 350-GHz compact range," Proc. SPIE Vol. 5427, p. 227-236, Algorithms for Synthetic Aperture Radar Imagery XI; Edmund G. Zelnio, Frederick D. Garber; Eds. September 2004.